Hornblende peridotite xenoliths from central Mexico reveal the highly oxidized nature of subarc upper mantle

Dawnika L. Blatter*
Ian S. E. Carmichael
Department of Geology and Geophysics, University of California, Berkeley, California 94720

ABSTRACT

Quaternary hornblende andesites have erupted along a fault zone near El Peñon, central Mexico. One of these flows contains 1–2 cm xenoliths of amphibole-rich spinel lherzolite and chromite websterite. These xenoliths are rare samples of subarc upper mantle from a region of continuing subduction, and they are the most oxidized mantle peridotites yet described (fayalite-magnetite-quartz +1.5 to 2.4). The abundant amphibole and high oxygen fugacities that characterize these xenoliths are significant because they provide direct evidence for metasomatism of the mantle wedge by slab-derived fluids. Phenocrysts of hornblende and lack of plagioclase phenocrysts in the host andesite indicate that it equilibrated with high water content (>8 wt%), and the presence of xenoliths implies rapid (26 km/day) ascent.

*E-mail: dblatter@uclink4.berkeley.edu.

INTRODUCTION

The dominant process in melt generation at convergent margins is fluxing of the mantle wedge by fluids from the down-going oceanic slab (Davies and Stevenson, 1992). This fluid oxidizes the mantle wedge and enriches it in volatile and large ion lithophile elements (Carmichael et al. 1996). Direct evidence for this type of metasomatism is limited because mantle xenoliths are rarely found in lavas or tephra associated with arc volcanism (Ertan and Leeman, 1996). Where arc-related ultramafic xenoliths are found, they are commonly hosted in alkaline rocks, like the backarc Simcoe alkali basalt of the Cascades (Leeman et al., 1990), and the basanites and alkali olivine basalts at Simberi Island in the Tabar-Lihir-Tanga-Feni arc (McInnes and Cameron, 1994). The few localities where ultramafic xenoliths are found in andesitic scoriae include Ichinomegata Crater in Japan (Tanaka and Aoki, 1981) and Moffett Volcano on Adak Island (Conrad and Kay, 1984). At Batan Island in the Philippines (Vidal et al. 1989), ultramafic xenoliths are found in andesitic scoriae and lava.

The El Peñon ultramafic xenoliths are the first to be discovered along the front of an active volcanic arc and are unusual because they occur in a hornblende andesite lava flow. This paper presents petrologic data on these xenoliths and discusses the implications of their unique geological context.

GEOLOGIC SETTING

The El Peñon andesite flow is located ~100 km southwest of Mexico City (Fig. 1). The oldest exposed rocks are Jurassic schists, capped by voluminous Oligocene to middle Miocene ash-flow tuffs from the Sierra Madre Occidental volcanic arc. Quaternary volcanism in this region marks the front of the Mexican Volcanic Belt and results from ongoing subduction of the Cocos plate beneath the North American plate (Nixon, 1982). The main axis of the Mexican Volcanic Belt is ~60 km to the northeast, where large stratovolcanoes such as Popocatépetl and Nevado

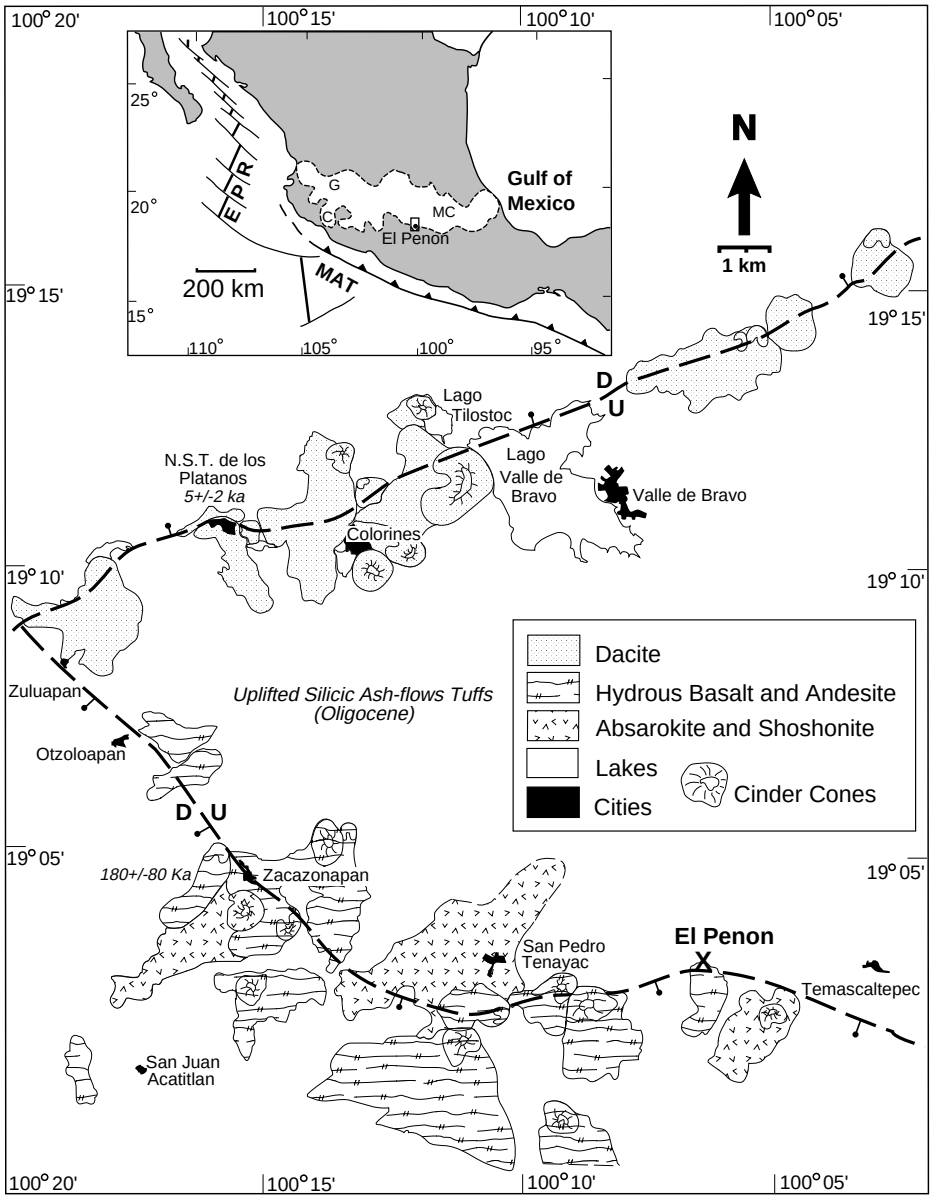

Figure 1. Quaternary volcanism in El Peñon area of central Mexico. Host andesite flow is marked X. Faults are bold dashed lines. Abbreviations in inset map are: G—Guadalajara, C—Colima, EPR—East Pacific Rise, MAT—Middle American Trench, and MC—Mexico City. Ages in italics determined at Berkeley Geochronology Center.

de Toluca dominate the landscape and are surrounded by shield volcanoes, cinder cones, lava flows, and silicic volcanic centers. In contrast, the sparse, small-volume flows and cones at El Peñon have erupted only along large faults amid the vast expanse of exposed basement rocks.

Prominent normal faults bound an uplifted block of Oligocene silicic ash-flow tuff (Fig. 1). The northern fault trends N75°E, and extends ~60 km along a river canyon. Dacites as young as 5.0 ± 2.0 ka have erupted along this fault, forming discrete, small volume flows. The southern fault truncates against the northern fault, extends 20 km to the southeast, and strikes N80°W. Displacement along this fault has created an escarpment that reaches 1000 m in places. Quaternary andesites, basaltic andesites, high-K andesites, and shoshonites have erupted along this escarpment forming small-volume flows that abut and overlap each other. The El Peñon flow (an andesite with augite, orthopyroxene, and hornblende phenocrysts) contains a variety of xenolithic material described below.

PETROLOGY

The xenoliths are uncommonly small (<2 cm) and fine grained (1 mm average grain size), making them difficult to recognize in the field. The 15 xenoliths analyzed for this study are type IV (deformed, cold peridotites) by the classification system summarized by Harte and Hawkesworth (1986). Most of the xenoliths are spinel lherzolite and chromium-olivine websterite, and about half contain modal hornblende (Table 1). Other xenolith varieties are harzburgite, pyroxenite, granitoid, megaxenocrysts (~2 cm) of unzoned diopside, and xenocrysts of quartz and plagioclase. Ultramafic xenolith textures are laminated porphyroblastic and granuloblastic, and the contacts between the xenoliths and the host consist of thin rims (generally one crystal width, ~200 μm) formed by crystals of hornblende and augite (Fig. 2). Some of the xenoliths have glassy veins where the host magma invaded them. Texturally and chemically, the xenoliths display evidence of metasomatism, including zones where the original minerals have been recrystallized or replaced with Cr-rich hornblende (Fig. 2). Several of the xenoliths have been oxidized sufficiently for spinel to be replaced by magnetite and hematite. This assemblage was oxidized prior to entrainment, because the host lava does not contain hematite. High olivine Mg#s distinguish these xenoliths from Alaskan-type ultramafic intrusions, and absence of serpentenization precludes derivation from an Alpine type ultramafic body. The textures and compositions of these xenoliths are consistent with an upper mantle source.

Microprobe analyses were performed on mineral phases for 15 different xenoliths; data from 5 representative varieties are presented in Table 1. For each xenolith, five grains of each mineral were analyzed at their cores and rims. In several xenoliths, diopside and orthopyroxene are replaced by patches of distinctively Cr-rich (>1 wt% Cr_2O_3) pargasitic hornblende. Olivine ranges from Fo_{89} in the lherzolites to Fo_{91} in the websterites, exhibiting no significant compositional difference between olivine cores and rims (ΔFo < 01). Orthopyroxene

TABLE 1. WET CHEMICAL BULK ANALYSIS OF Z-509 AND REPRESENTATIVE ELECTRON MICROPROBE ANALYSES OF Z-509 & XENOLITHS X4, X6, X8, X12 & X14

Sample	Composition	Modes	SiO_2	TiO_2	Al_2O_3	Cr_2O_3	Fe_2O_3	FeO	MnO	NiO	MgO	CaO	Na_2O	K_2O	Total	T_{BKN} (°C)	Δ FMQ
Z-509	*host andesite*															1020	+2.5*
	bulk analysis		58.75	0.97	16.11		2.16	3.34	0.10		4.14	6.80	3.60	1.90	98.11		
opx core	$Wo_{02}En_{81}Fs_{17}$	03	54.30	0.21	1.58			11.66	0.21		30.53	1.05	0.00	0.00	99.49		
opx rim	$Wo_{02}En_{79}Fs_{19}$		53.93	0.26	1.82			12.56	0.25		30.00	1.02	0.00	0.00	99.83		
aug core	$Wo_{42}En_{49}Fs_{09}$	08	52.92	0.31	1.78	0.23		5.82	0.18		17.37	20.60	0.35	0.00	99.37		
aug rim	$Wo_{43}En_{46}Fs_{11}$		50.85	0.83	3.17			6.97	0.24		15.62	20.50	0.44	0.00	98.93		
hbl core		09	44.89	2.00	10.96	0.08		8.86	0.11		16.71	11.14	2.62	0.55	97.92		
hbl rim			43.00	2.31	12.30	0.12		10.62	0.14		15.21	11.24	2.40	0.66	98.00		
aug gms	$Wo_{42}En_{45}Fs_{13}$	08	51.09	0.62	3.13	0.03		7.65	0.24		15.22	19.96	0.48		98.41		
plag gms	$Ab_{40}An_{59}Or_{01}$	28	51.43		29.06			0.81				12.13	4.52	0.25	98.59		
ti-mt		10	0.14	15.19	1.08	0.04	40.84	36.17	0.44		1.80	0.17	0.02		95.87		
glass		34	77.13	0.68	11.58	0.01		1.02	0.04	0.01	0.03	0.20	1.47	5.74	98.06		
X4	*hbl-sp lherz*															853 ± 17	+1.5
olv core	$Fo_{89}Fa_{11}$	37	40.57		0.00	0.03		10.71	0.14	0.32	47.52	0.03			99.33		
opx core	$Wo_{01}En_{89}Fs_{10}$	40	56.50	0.05	2.15	0.16		6.97	0.19		33.60	0.35	0.01	0.01	99.98		
diop core	$Wo_{48}En_{48}Fs_{04}$	16	53.08	0.17	2.30	0.25		2.66	0.08		17.07	23.55	0.08	0.01	99.25		
Cr-spinel	Cr# = 0.24	04	0.01	0.23	42.02	20.06	7.78	12.07	0.13	0.30	17.16	0.01			99.14		
Cr-hbl		03	43.45	0.64	14.16	1.20		4.49	0.06		17.75	11.70	2.46	0.22	96.14		
X6	*cr-olv web*															969 ± 17	+2.2
olv core	$Fo_{91}Fa_{09}$	32	40.86		0.01	0.00		8.41	0.03	0.37	49.51	0.02			99.26		
opx core	$Wo_{00}En_{92}Fs_{08}$	46	58.29	0.01	0.12	0.14		5.54	0.12		35.28	0.08	0.01	0.01	99.62		
diop core	$Wo_{45}En_{51}Fs_{04}$	19	53.98	0.11	1.65	0.28		2.45	0.09		18.38	22.52	0.33	0.01	99.80		
chromite	Cr# = 0.79	03	0.01	0.08	9.79	53.14	8.16	17.75	0.21	0.11	10.04	0.00			98.56		
X8	*hbl-cr-olv web*															953 ± 17	+2.4
olv core	$Fo_{91}Fa_{09}$	20	41.52		0.00	0.02		8.39	0.10	0.41	49.98	0.00			100.41		
opx core	$Wo_{00}En_{92}Fs_{08}$	50	57.89	0.01	0.14	0.06		5.61	0.13		35.88	0.08	0.00	0.00	99.79		
diop core	$Wo_{46}En_{51}Fs_{03}$	22	54.35	0.08	2.12	0.17		2.29	0.05		18.63	22.58	0.24		100.28		
chromite	Cr# = 0.72	05	0.01	0.15	12.95	50.31	7.33	18.15	0.23	0.13	10.12	0.00			98.74		
Cr-hbl		03	44.44	1.13	11.56	1.63		5.20	0.11		18.14	10.87	2.99	0.68	96.90		
X12	*hbl-sp lherz*															791 ± 17	+1.6
olv core	$Fo_{89}Fa_{11}$	37	40.84		0.00	0.02		11.09	0.15	0.36	47.94	0.01			100.41		
opx core	$Wo_{01}En_{88}Fs_{11}$	30	57.07	0.05	2.38	0.27		7.19	0.15		33.49	0.37	0.01	0.01	100.98		
diop core	$Wo_{46}En_{51}Fs_{03}$	18	54.35	0.08	2.12	0.24		1.96	0.04		18.32	22.91	0.28	0.01	100.31		
Cr-spinel	Cr# = 0.20	07	0.01	0.15	45.66	16.56	7.57	11.30	0.12	0.34	17.93	0.06			99.06		
Cr-hbl		08	43.69	0.70	14.22	1.04		4.39	0.06		18.17	11.80	2.53	0.22	96.90		
X14	*sp lherz*															930 ± 17	+2.1
olv core	$Fo_{91}Fa_{09}$	35	40.81		0.00	0.02		9.02	0.13	0.39	48.73	0.05			99.14		
opx core	$Wo_{01}En_{89}Fs_{10}$	41	55.81	0.07	3.65	0.30		6.29	0.14		33.45	0.63	0.02	0.00	100.37		
diop core	$Wo_{47}En_{48}Fs_{05}$	21	52.76	0.23	3.71	0.40		3.18	0.09		16.68	22.53	0.50	0.01	100.04		
Cr-spinel	Cr# = 0.19	03	0.03	0.11	46.24	16.10	7.50	11.23	0.13	0.39	18.02	0.02			99.12		

Note: 5 points per mineral grain were averaged for each analysis. A Cameca SX-50 electron microprobe was used with a focused beam at 15 kV and 20 nA for 10-40 s count times. Abbreviations are opx (orthopyroxene), aug (augite), hbl (hornblende), plag (plagioclase), ti-mt (titanomagnetite), gms (groundmass), olv (olivine), diop (diopside), Cr-spinel (chromium spinel), Cr-hbl (chromium hornblende), sp (spinel), lherz (lherzolite), cr (chromite), and web (websterite). Cr# = Cr/(Cr + Al). Modes are in volume % for ~500 pounts counted. Spinels were analyzed using secondary standards (Ionov and Wood, 1992) and recalculated by stoichiometry. The Fe^{3+}/Fe^{total} value for each unknown spinel analysis was corrected additively by the mean value of $(Fe^{3+}/Fe^{total})_{true} - (Fe^{3+}/Fe^{total})_{probe}$, which was +0.01 for the chromites and -0.01 for the Cr-spinels. V_2O_3 was analyzed in spinels and ranges from 0.06 to 0.15 wt %. T_{BKN} = temperature calculated using Brey and Kohler (1990) from coexisting pyroxene core compositions, assuming pressure (P) = 15 kbar (for consistency with other published calculations). Delta fayalite magnetite quartz (ΔFMQ) values were calculated at T_{BKN} and P = 15 kbar, using the methods of Wood et al (1990).
*Calculated using Kress and Carmichael (1991).

ranges from $Wo_{01}En_{88}Fs_{11}$ to $Wo_{01}En_{89}Fs_{10}$, and Al_2O_3 = 2.15–3.65 wt% in the lherzolites to $Wo_{00}En_{92}Fs_{08}$, and Al_2O_3 < 0.14 in the websterites; Al_2O_3 concentrations decrease slightly in the rims. Clinopyroxene is diopsidic with Ca-enriched rims, and lower Cr_2O_3 (<0.40 wt%) than that of diopside in other type IV xenoliths (Luhr and Aranda-Gomez, 1997). Diopside in the lherzolites is slightly more Ca rich than in the websterites. Cr-spinel in the lherzolites have Cr_2O_3 ranging from 16 to 20 wt%, and chromite (~50–53 wt% Cr_2O_3) occurs in the websterites. Megaxenocrysts (~1 cm) of Cr-poor diopside ($Wo_{48}En_{34}Fs_{18}$) occur that are more Ca and Fe rich than augite megaxenocrysts from alkali olivine basalts (Righter and Carmichael, 1993).

The host andesite contains phenocrysts of orthopyroxene, augite, and hornblende, commonly in glomeroporphyritic clusters in a groundmass of augite, plagioclase, titanomagnetite, and glass. The orthopyroxene phenocrysts have very little variation between the cores ($Wo_{02}En_{81}Fs_{17}$) and rims ($Wo_{02}En_{79}Fs_{19}$). Augite phenocryst rims are enriched in Ca and Fe ($Wo_{43}En_{46}Fs_{11}$) with respect to their cores ($Wo_{42}En_{49}Fs_{09}$); with the exception of a few crystals that appear to have nucleated on preexisting cores of Fe-rich diopside ($Wo_{46}En_{36}Fs_{18}$). Pargasitic hornblende phenocrysts contain twice the iron and much less Cr_2O_3 (0.04 wt%) than the hornblende in the xenoliths, and have 15–30 μm black dehydration rims. The hornblende and augite that encapsulate the xenoliths have the same compositions as the phenocrysts of hornblende and augite in the andesite (Fig. 2).

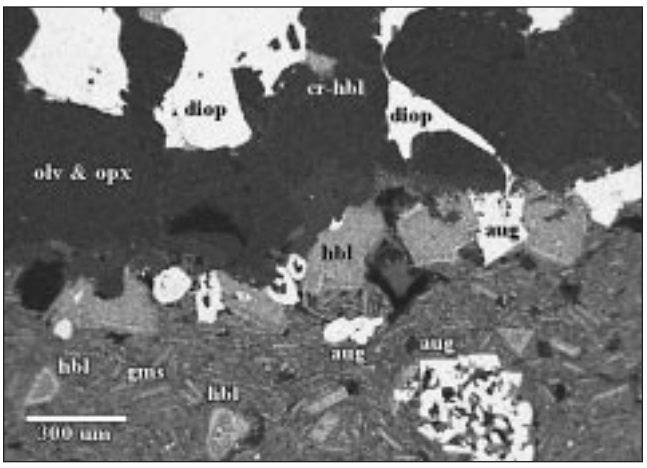

Figure 2. Calcium X-ray map of margin of xenolith X4. High-calcium phases appear light and low-calcium phases appear dark. Xenolith covers top half of image and is made of opx (orthopyroxene), olv (olivine), diop (diopside), and cr-hbl (chromium-rich hornblende). Rim is in middle of image and is made of aug (augite) and hbl (hornblende) that have same compositions as aug and hbl phenocrysts in host lava, which is shown in bottom half of image (gms = groundmass).

OXYGEN FUGACITY

High oxygen fugacity (fO_2) was discussed by Brandon and Draper (1996) as one of the characteristics associated with subduction-related metasomatism in the subarc mantle. Their study determined that xenoliths from Simcoe, Washington formed at fayalite-magnetite-quartz (FMQ) +0.3 to +1.4 log units. A similar study of subarc ultramafic xenoliths from Ichinomegata, Japan (Wood and Virgo, 1989) yielded fO_2s of FMQ to FMQ + 1.2. Following the methods of Wood et al. (1990), fO_2s were calculated for the El Peñon xenoliths from core compositions of coexisting orthopyroxene, olivine, and spinel from the center of each nodule. Temperatures were calculated by Brey and Kohler's (1990) two-pyroxene method and 15 kbar of pressure was assumed (Table 1). The fO_2 of the host lava was calculated using the ferric-ferrous ratio of the bulk rock (xenolithic material excluded) and the calibration of Kress and Carmichael (1991).

The fO_2s calculated for the El Peñon xenoliths are higher than any previously published, ranging from FMQ +1.5 to +2.4 log bar units (Table 1 and Fig. 3A). Considering that a similar range of fO_2s is found in western and central Mexican basaltic andesites and hornblende andesites (including the host andesite with fO_2 = FMQ +2.5 [Fig. 3B]), the high xenolith fO_2 values support the postulate that lavas inherit fO_2s from their source regions (Carmichael, 1991). However, the El Peñon ultramafic xenoliths are not oxidized enough to account for the high fO_2s (FMQ +3 to +5) of phlogopite-bearing lamprophyric lavas found in western Mexico (Carmichael et al. 1996).

DISCUSSION

Because the hornblende and augite that rim the xenoliths have compositions nearly identical to the hornblende and augite phenocrysts in the host andesite, it follows that the xenoliths were entrained under the pressure-temperature (*P-T*) conditions of phenocryst growth. Water-saturated phase-equilibria experiments have been done on a Paricutin andesite, which has nearly the same bulk composition as the El Peñon andesite (Eggler, 1972). According to Eggler's data, the phenocryst assemblage of El Peñon andesite (orthopyroxene, augite, and hornblende) is stable at T < ~950 °C and P = 4.3–10 kbar (the upper limit of the data), with >8 wt% H_2O (Moore et al., 1998). Had the host andesite grown phenocrysts at <4.3 kbar, plagioclase would be present as a phenocryst, and higher temperatures would result in absence of hornblende. The high-pressure phenocryst assemblage of the lava is consistent with entrainment of upper mantle xenoliths and rapid eruption from depth, instead of storage in the shallow crust before eruption.

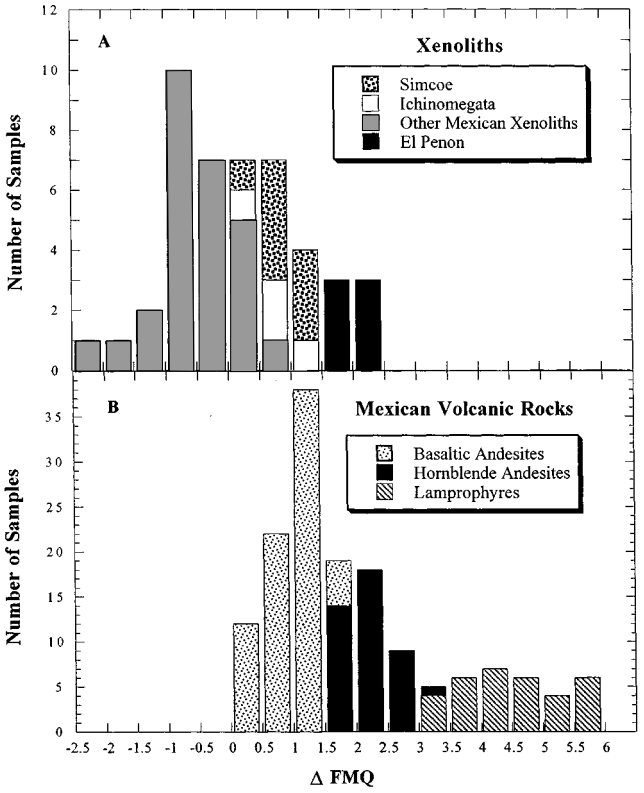

Figure 3. A: Frequency distribution plot of oxygen fugacity (fO_2) values for mantle xenoliths from El Peñon, central Mexico; other Mexican localities (Luhr and Aranda-Gomez, 1997); Simcoe, Washington (Brandon and Draper, 1996); and Ichinomegata, Japan (Wood and Virgo, 1989). All fO_2s for this plot were calculated by methods of Wood et al. (1990) and are reported relative to FMQ (fayalite-magnetite-quartz) buffer. El Peñon xenolith fO_2s average one log unit higher than all other published values. B: Histogram of fO_2s from partially glassy Mexican lavas and scoria (Carmichael, 1991). Note that hornblende andesites have an fO_2 range similar to that of El Peñon xenoliths.

The preservation of the ultramafic xenoliths throughout the ascent and eruption of the host lava is remarkable, because dissolution experiments have shown that peridotite xenoliths are only preserved in their host magmas for several hours (Scarfe and Brearley, 1987). The rim-forming augite and hornblende may have armored the xenoliths and slowed dissolution substantially as is documented in the case of augite rims armoring quartz xenocrysts (Donaldson, 1985). Rapid ascent and eruption of the host magma are also essential in the preservation of the xenoliths. The minimum ascent rate of the host magma has been calculated using Stoke's settling velocity equation and the following assumptions: the density of the magma is 2122 kg/m^3 (calculated using the volume equation and data summarized in Lange [1994], with 8 wt% H_2O and volume data from Ochs and Lange [1997]; P = 10 kbar, and from two-pyroxene thermometry, T = 1020 °C); xenolith radius = 1 cm; xenolith density = 3250 kg/m^3; and the viscosity of the magma = 82 P (calculated following Shaw, 1972). Because the xenoliths have small radii (<2 cm), the effect of the density difference between the xenoliths and the magma is small, and the effect of magma viscosity is maximized. The result is a minimum ascent velocity of 26 km/day, yielding a transit time through the crust of <2 days. Under these estimates, xenoliths >2 cm would have settled and dissolved until they became small enough to be transported by the ascending magma. Incorporation of cooler wall rock may have caused precipitation of phenocrysts in the host magma, allowing the dissolving xenoliths to be encapsulated by phenocryst rims, protecting the xenoliths from further dissolution. This was followed by rapid ascent and eruption of the El Peñon andesite, which quenched at the surface, preserving the mantle xenoliths it had entrained and the high-P phase assemblage of nearly unzoned phenocrysts. The paucity of plagioclase microphenocrysts as well as the presence of hornblende phenocrysts, having only thin (<30 μm) dehydration rims indicate that the magma retained enough water to suppress crystallization of plagioclase and stabilize hornblende until the andesite erupted.

SUMMARY

The mantle beneath El Peñon was metasomatized by subduction-related fluids, causing hydration and oxidation of the original mantle material. Evidence for this process is found in many of the El Peñon xenoliths where pyroxene is replaced with Cr-rich hornblende. In addition, high fO_2s (FMQ + 2.4) have been imprinted and recorded in the spinels, some of which have been locally oxidized to magnetite and hematite. The host andesite phenocryst assemblage indicates equilibration at lower crustal or upper mantle depths and hydrous conditions.

ACKNOWLEDGMENTS

Support by National Science Foundation grants EAR-94-18105 and EAR-94-06129 to Carmichael. A. Carmichael, R. McPhail, M. Escobar, and K. Fillmore provided help in the field; Peter McIntyre assisted in sample preparation. We thank Andy Robinson for providing spinel standards. Thoughtful reviews by T. W. Sisson and W. P. Leeman improved this paper considerably.

REFERENCES CITED

Brandon, A. D., and Draper, D. S., 1996, Constraints on the origin of the oxidation state of mantle overlying subduction zones: An example from Simcoe, Washington, USA: Geochimica et Cosmochimica Acta, v. 60, p. 1739–1749.

Brey, G. P., and Kohler, T., 1990, Geothermobarometry in four-phase lherzolites II: New thermobarometers, and practical assessment of existing thermobarometers: Journal of Petrology, v. 31, p. 1353–1378.

Carmichael, I. S. E., 1991, The redox states of basic and silicic magmas: A reflection of their source regions?: Contributions to Mineralogy and Petrology, v. 106, p. 129–141.

Carmichael, I. S. E., Lange, R. A., and Luhr, J. F., 1996, Quaternary minettes and associated volcanic rocks of Mascota, western Mexico: A consequence of plate extension above a subduction modified mantle wedge: Contributions to Mineralogy and Petrology, v. 124, p. 302–333.

Conrad, W. K., and Kay, R. W., 1984, Ultramafic and mafic inclusions from Adak Island: Crystallization history, and implications for the nature of primary magmas and crustal evolution in the Aleutian Arc: Journal of Petrology, v. 25, p. 88–125.

Davies, J. H., and Stevenson, D. J., 1992, Physical model of source region of subduction zone volcanics: Journal of Geophysical Research, v. 97, p. 2037–2070.

Donaldson, C. H., 1985, The rates of dissolution of olivine, plagioclase, and quartz in a basalt melt: Mineralogical Magazine, v. 49, p. 683–693.

Eggler, D. H., 1972, Water-saturated and undersaturated melting relations in a Paricutin andesite and an estimate of water content in the natural magma: Contributions to Mineralogy and Petrology, v. 34, p. 261–271.

Ertan, I. E., and Leeman, W. P., 1996, Metasomatism of Cascades subarc mantle: Evidence from a rare phlogopite orthopyroxenite xenolith: Geology, v. 24, p. 451–454.

Harte, B., and Hawkesworth, D. J., 1986, Mantle domains and mantle xenoliths, *in* O'Reilly, S. Y., ed., Fourth International Kimberlite Conference, Volume 2: Kimberlites and related rocks: Perth, Australia, Geological Society of Australia, Blackwell Scientific Publications, p. 649–686.

Ionov, D. A., and Wood, B. J., 1992, The oxidation state of subcontinental mantle: Oxygen thermobarometry of mantle xenoliths from central Asia: Contributions to Mineralogy and Petrology, v. 111, p. 179–193.

Kress, V. C., and Carmichael, I. S. E., 1991, The compressibility of silicate liquids containing Fe_2O_3 and the effect of composition, temperature, oxygen fugacity, and pressure on their redox states: Contributions to Mineralogy and Petrology, v. 108, p. 82–92.

Lange, R. A., 1994, The effect of H_2O, CO_2, and F on the density and viscosity of silicate melts, *in* Carroll, M. R., and Holloway, J. R., eds., Volatiles in magmas: Mineralogical Society of America Reviews in Mineralogy, v. 30, p. 331–365.

Leeman, W. P., Smith, D. R., Hildreth, W., Palacz, Z., and Rogers, N., 1990, Compositional diversity of late Cenozoic basalts in a transect across the southern Washington Cascades: Implications for subduction zone magmatism: Journal of Geophysical Research, v. 95, p. 19561–19582.

Luhr, J. F., and Aranda-Gomez, J. J., 1997, Mexican peridotite xenoliths and tectonic terranes: Correlations among vent location, texture, temperature, pressure, and oxygen fugacity: Journal of Petrology, v. 38, p. 1075–1112.

McInnes, B. I. A., and Cameron, E. M., 1994, Carbonated, alkaline hybridizing melts from a sub-arc environment: Mantle wedge samples from the Tabar-Lihir-Tanga-Feni arc, Papua New Guinea: Earth and Planetary Science Letters, v. 122, p. 125–141.

Moore, G., Vennemann, T., and Carmichael, I. S. E., 1998, An empirical model for the solubility of H_2O in magmas to 3 kilobars: American Mineralogist, v. 83, p. 36–42.

Nixon, G. T., 1982, The relationship between Quaternary volcanism in central Mexico and the seismicity and structure of subducted ocean lithosphere: Geological Society of America Bulletin, v. 93, p. 514–523.

Ochs, F. A., III, and Lange, R. A., 1997, The partial molar volume, thermal expansivity, and compressibility of H_2O in $NaAlSi_3O_8$ liquid: New measurements and an internally consistent model: Contributions to Mineralogy and Petrology, v. 129, p. 155–165.

Righter, K., and Carmichael, I. S. E., 1993, Megaxenocrysts in alkali olivine basalts: Fragments of disrupted mantle assemblages: American Mineralogist, v. 78, p. 1230–1245.

Scarfe, C. M., and Brearley, M., 1987, Mantle xenoliths: Melting and dissolution studies under volatile-free conditions, *in* Nixon, P. H., ed., Mantle xenoliths, Volume 1: Chichester, John Wiley & Sons, p. 599–608.

Shaw, H. R., 1972, Viscosities of magmatic silicate liquids: An empirical method of prediction: American Journal of Science, v. 272, p. 870–893.

Tanaka, T., and Aoki, K.-I., 1981, Petrogenic implications of REE and Ba data on mafic and ultramafic inclusions from Itinome-gata, Japan: Journal of Geology, v. 89, p. 369–390.

Vidal, P., Dupuy, C., Maury, R., and Richard, M., 1989, Mantle metasomatism above subduction zones: Trace element and radiogenic isotope characteristics of peridotite xenoliths from Batan Island (Philippines): Geology, v. 17, p. 1115–1118.

Wood, B. J., and Virgo, D., 1989, Upper mantle oxidation state: Ferric iron contents of lherzolite spinels by ^{57}Fe Mossbauer spectroscopy and resultant oxygen fugacities: Geochimica et Cosmochimica Acta, v. 53, p. 1277–1291.

Wood, B. J., Bryndzia, L. T., and Johnson, K. E., 1990, Mantle oxidation state and its relationship to tectonic environment and fluid speciation: Science, v. 248, p. 337–344.

Manuscript received March 23, 1998
Revised manuscript received July 28, 1998
Manuscript accepted August 4, 1998